Rev. Adv. Mater. Sci. 48 (2017) 170-178

RELAXATION PHENOMENA IN DISCLINATED MICROCRYSTALS

A.E. Romanov[1,2,3], A.L. Kolesnikova[1,2,4], I.S. Yasnikov[1], A.A. Vikarchuk[1], M.V. Dorogov[1], A.N. Priezzheva[1], L.M. Dorogin[1,2] and E.C. Aifantis[1,2,5]

[1]Togliatti State University, 445020 Togliatti, Russia
[2]ITMO University, 197101 St. Petersburg, Russia
[3]Ioffe Institute RAS, 194021 St. Petersburg, Russia
[4]Institute of Problems of Mechanical Engineering RAS, 199178 St. Petersburg, Russia
[5]Aristotle University of Thessaloniki, GR 54124 Thessaloniki, Greece

Received: February 21, 2017

Abstract. Disclinated microcrystals (DMCs) can be obtained in the form of decahedrons, icosahedrons, and pentagonal prisms. We present results of metallic DMC fabrication by employing the process of electrodeposition. We further provide experimental evidence of structural transformations in DMCs during electrodeposition and heat treatment. We propose a model of DMC in the framework of continuum mechanics and discuss some typical results for calculations of the stresses and internal energy for elongated and sphere-like crystalline objects containing either one or six disclinations, or a distributed spherical disclination. Relaxation of mechanical stresses caused by disclinations leads to structural transformations in DMCs. We review the existing models of stress relaxation in DMCs and discuss new models of stress relaxation through dislocation loops or additional disclination ensembles in the DMC interior or lattice mismatched shells formed on the DMC surface.

1. INTRODUCTION

Nowadays it is well-established that physical and mechanical properties of solids are size-dependent. The size-dependence has been attributed to material non-uniformities, stochastic effects, and gradients of various physical fields, as observed in a variety of materials and processes ranging from nano/micro and meso/macro to mega/giga scales. Early and more recent discussions of this topic can be found in Refs. [1(a-c)] and works quoted therein. The size effects can be found more pronounced in nano and microcrystalline objects – for comprehensive reviews see Refs. [2-9]. One remarkable structural feature of such objects is the presence of five-fold symmetry in individual small particles (the first publications on this subject are dated back to the mid-1960's [10,11]) and in the local arrangement of grains in polycrystals [12,13].

We focus on the micro-objects having shapes of a decahedron, a pentagonal prism and an icosahedron, therefore having either one or six axes of pentagonal symmetry. Such crystalline pentagonal particles (PPs) and rods (PRs) are usually fabricated from materials with FCC crystal structure such as Cu, Ag, Au, Si, C *etc.*; *e.g.* see reviews [14-21] and some recent works [22-30]. In the process of FCC crystal growth low-energy {111}-type twin boundaries (TBs) can be formed in the material interior. In pentagonal micro-objects TBs are arranged in special configurations providing the observed five-fold symmetry, and this is why PPs and PRs are sometimes referred to as "multiple twinned" [14-16]. Another important feature of pentagonal micro-objects

Corresponding author: A.E. Romanov, e-mail: alexey.romanov@niuitmo.ru

is the crystallography of their surface; decahedral and icosahedral particles are bounded by {111}-type crystallographic facets and pentagonal prisms have {100}-type crystallographic planes as side facets, as well as {111}-type planes as cap facets [16]. This specific crystallography was also shown to be responsible for enhanced catalytic activity of pentagonal micro-objects [18]. Finally, as it was originally pointed out in Refs. [31,32], pentagonal microcrystals contain disclinations – specific defects of rotational type (for a review on the properties of disclinations, see Ref. [33]). Therefore, pentagonal micro-objects can be also classified as disclinated microcrystals (DMCs). In the following, we will employ this notation to underline the role of disclinations in the properties of PPs and PRs.

In this paper, we first present results of DMC fabrication in the process of electrodeposition of metals. In particular, we demonstrate that the parameters of electrodeposition, such as temperature and pH of electrolyte, electric current and voltage strongly influence the morphology and internal structure of DMCs. We also provide experimental evidence of structural transformations in DMCs during electrodeposition and heat treatment, namely, the appearance of internal cavities and pores, as well as the formation of outgrowths (or extrusions) at copper icosahedral particles and pentagonal prisms. Second, we consider a model of DMC and present some results on calculation of stresses and internal energy for elongated and sphere-like crystalline objects containing either one or six disclinations, or a distributed spherical disclination. Relaxation of mechanical stresses due to disclinations is realized via structural transformations in DMCs. We thus review existing models of stress relaxation in DMCs [16,34]. We also discuss new models of stress relaxation based on the formation of additional disclination ensembles at DMC subsurface layers and the nucleation of dislocation loops near the surface of DMCs.

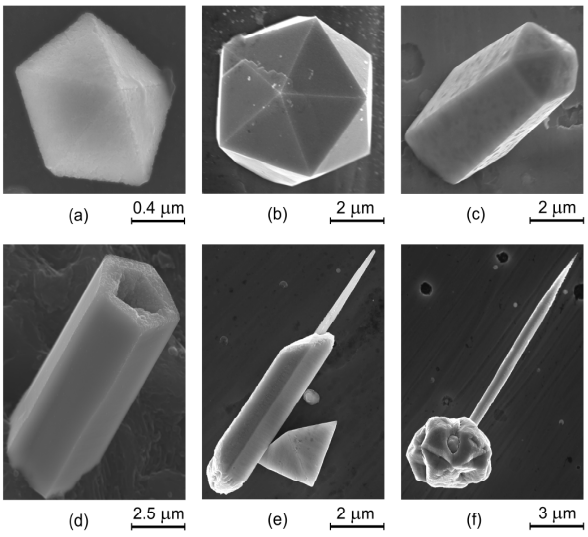

Fig. 1. DMCs with perfect (a - c) and defective (d - f) exterior shapes: decahedral (a) and icosahedral (b) silver particles; pentagonal prismatic copper rod without (c) and with (d) hole inside and copper outgrowth/extrusion from the PR (e) and PP (f).

2. EXPERIMENTAL BACKGROUND

In this section we consider some results of experimental studies of nano and microscale disclinated particles received by electrodeposition of copper and silver in Togliatti State University, Russia (Figs. 1-3).

In Fig. 1 pentagonal Ag microparticles (a-b) and Cu microrods (c) are depicted. These particles have perfect shape, but this does not mean that they do not contain numerous internal defects. Fig. 1 also shows microparticles with a defective external shape: PR with hole inside (d) and outgrowth emerging from the copper particle (e-f) [19,23,35]. These imperfections originate during the electrodeposition process.

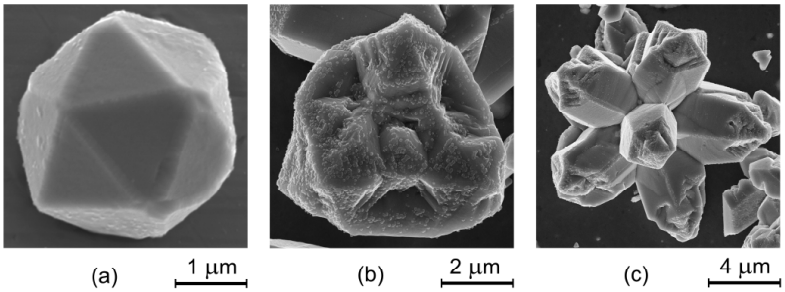

Fig. 2. Transformation of the habit/morphology of copper icosahedral microcrystals with six fivefold symmetry axes at concentrations (a) 0, (b) 1.0, (c) 2.0 g/L of the KBr inhibitor added to the standard sulfuric electrolyte (adapted from [36]).

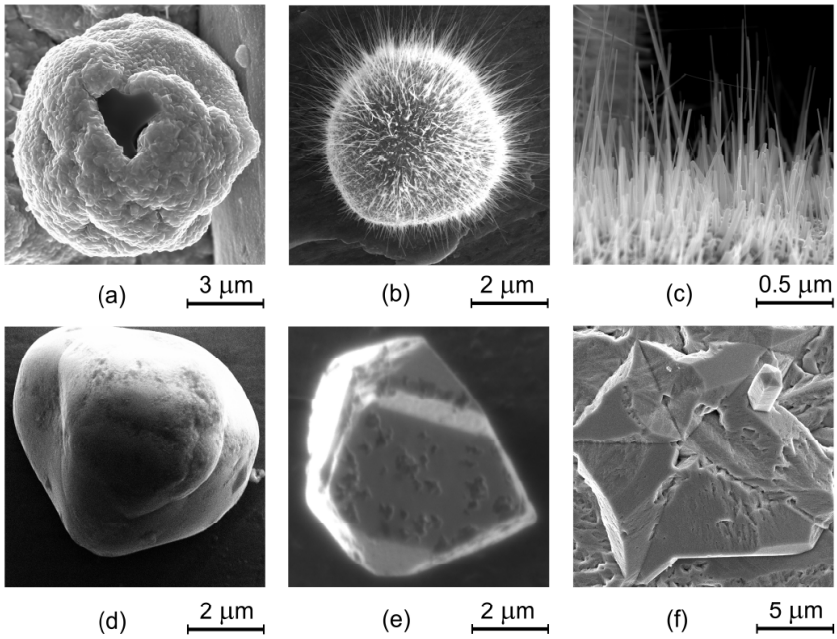

Fig. 3. Copper disclinated microcrystals (DMCs) with different habitus, configuration or morphology: (a) formation of the cavities and (b-c) growth of numerous whiskers in DMC after heating to 400 °C in air; (d) loose faceting in DMC after heating to 700 °C in vacuum; (e) internal cavities in DMC; (f) micro-PR growing from the places of TBs junctions.

The essential role of experimental parameters such as electrolyte temperature and chemical composition, potentiostatic or galvanostatic conditions of deposition was higlighted in papers [6,23,28]. In particular, increasing the pH value of electrolyte from acidic to alkali solution caused the change of microcrystal habitus/configuration from strongly distorted shape, through regularly faceted shape to a smooth one for electrodeposited small Ag particles and microcrystals [28]. In addition, in [36] it was demonstrated demonstrated the transformation of the habit morphology of icosahedral pentagonal microcrystals at different concentrations of the KBr inhibitor added to the standard sulfuric copper-coating electrolyte and fixed electrodeposition time (Fig. 2). As we can see this leads to the growth of PRs on the surface of the initial icosahedron.

Electrodeposition of particles with subsequent heating to 400°C and above in air, leads to the formation of cavities (Fig. 3a) and channels and the growth of numerous whiskers (Figs. 3b and 3c) outside of initially outwardly perfect particles [37]. Similar way heating in vacuum causes microparticles to lose faceting and no whiskers are observed (Fig 3d). The holes and empty channels are formed during the PP and PR growth (Fig. 3e). It can be observed the formation of outgrowths or extrusions from the particle, accompanied by the formation of internal cavities in the particle (Fig. 3f). In this connection, it is also worth mentioning that outgrowths emerging near the places of TBs junctions, are often pentagonal (Fig. 3f), *i.e.* they are micro-PRs.

The experimental data described above suggest that under the influence of elastic stress fields associated with disclination type defects, the external shape and configuration/morphology of small particles and microcrystals can be modified. We will discuss the possible channels or modes of relaxation of stresses and associated diminishing of elastic energy in Section 4.

3. MODELING OF DISCLINATED MICROCRYSTALS

The origin of pentagonal symmetry in PRs and PPs is illustrated in the schematics given in Fig. 4. As shown in Fig. 4a, PR is a polycrystal consisting of five FCC monocrystalline regions divided by five TBs. Lateral faces of this multiple-twinned PR are crystallographic planes of {100}-type, whereas cup faces are of {111}-type. The axis of fivefold symmetry is parallel to <100>-type direction. The internal structure of PRs can be understood from the schematics of Figs. 4b and 4c [31]. In Fig. 4b, five undistorted parts of the PR are aligned along four TBs, which in FCC crystals are {111}-type planes; see, for ex-

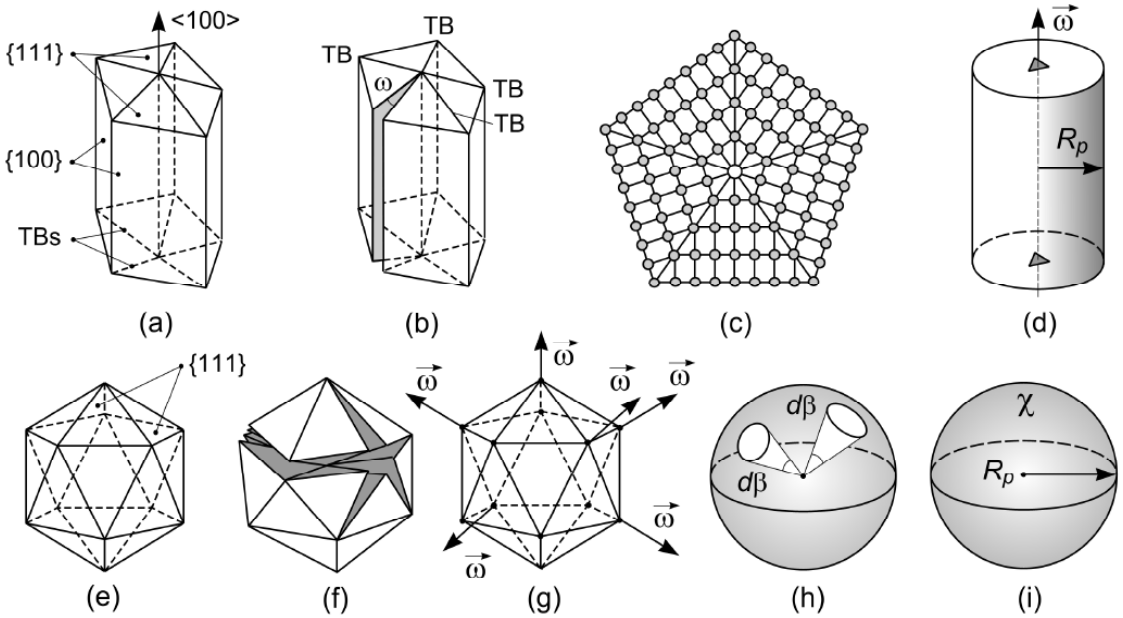

Fig. 4. Disclination models for DMCs: (a) PR with internal twin boundaries; (b) angular gap ω in a PR; (c) twinned crystal lattice of PR; (d) PR modeled as cylinder of radius R_p having positive wedge disclination of strength ω; (e) icosahedral PP; (f) PP with solid angle deficiency; (g) PP with six wedge disclinations of strength ω; (h) PP with infinitesimal solid cones $d\beta$; and (i) PP modeled as spheroid with distributed Marks–Yoffe disclination.

ample, Ref. [16]. Because of FCC crystal geometry there is a small angular gap preventing the formation of a completely connected and undistorted PR. This angular gap however can be eliminated by mutual rotation of the gap faces with the formation of a fifth TB. The closing of the gap is equivalent to the introduction of a positive wedge disclination along the PR axis [31,38]. The resulting configuration of the crystal lattice in the PR cross-section (which is the plane of the {110}-type) is shown in Fig. 4c where a triangle designates a wedge disclination. In the case of PPs, the standard morphology is that of an icosahedron with {111}-type crystallographic facets only [34,39]. The icosahedron possesses six disclinations shown in Fig. 4e. It has been proven [34] that each fivefold axis, which appears at the junction of five twin boundaries in a PR or a PP, contains a positive wedge disclination of the strength $\omega=2\pi - 10\arcsin(1/\sqrt{3}) \approx 7°20'$.

The introduction of the disclinations leads to elastic distortions of the crystal lattice in the bulk of the PR and PP. Within a continuum mechanics model, which is suitable for the calculation of elastic fields and energies, a PR can be described as an elastic cylinder with a coaxial positive wedge disclination (Fig. 4d) and a PP can be described as an elastic spheroid with six positive wedge disclinations (Fig. 4g) or with one distributed Marks-Yoffe disclination (Fig. 4i) [39]. Summarizing all the above, one can conclude that in order to describe the elastic properties of the pentagonal faceted particles it is convenient to use the configuration of a disclinated cylinder or a disclinated spheroid.

The characteristics and properties of disclinations, which distinguish them from dislocations, are important in our theoretical model. Namely, the elastic strains and stresses of a single straight disclination diverge away from the disclination line. Disclination energy increases quadratically with increasing characteristic screening parameter, such as crystallite size (more details on disclinations in crystals are given in the book chapter [38]). In this regard, straight-line disclinations can only exist in crystals of small size or in the presence of other defects that can reduce (screen) their elastic fields. Such properties of disclinations in finite size bodies are the cause for the manifestation of various mechanisms of mechanical stress relaxation in PRs and PPs.

There exist a number of models of stress relaxation in disclinated crystals. In the following section we briefly describe the developed models of stress relaxation related to pentagonal crystals

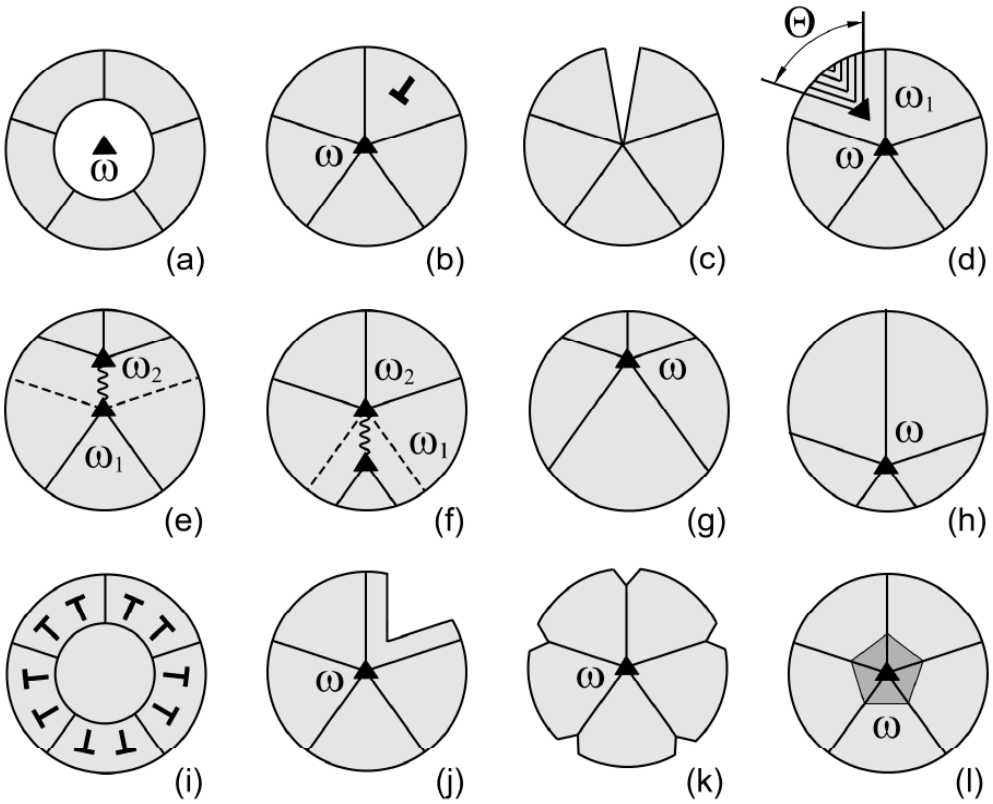

Fig. 5. Relaxation processes in DMCs: (a) appearance of empty channel; (b) formation of a straight-line dislocation; (c) opening of a gap; (d) appearance of a negative disclination with a system of stacking faults; (e, f) decomposing the disclination into two others linked by a "disclinational" stacking fault; (g, h) shifting of the pentagonal axis towards the periphery; (i) formation of a region without a disclination; (j) formation of an open sector outside TBs; (k) faceting of surface near the TBs; (l) faceting the surface around the disclination axis.

[16,33,34] and present a new model of stress relaxation, which explains the simultaneous formation of an "outgrowth" on the surface and a "cavity" inside the interior of a disclinated crystal.

4. RELAXATION PROCESSES IN DISCLINATED MICROCRYSTALS

Over the past two decades a number of models of stress relaxation in PRs and PPs has been proposed. Fig. 4 presents the schematics of these models. The energy criterion that triggers the relaxation process is of the usual form $E_{initial} \geq E_{final}$, where $E_{initial}$ and E_{final} are the energies of DMCs before and after relaxation.

It has been shown that the following processes contribute to the diminishing of elastic energy in DMCs: appearance of an empty channel/hole (Fig. 5a) [35,38,40]; formation of a straight-line dislocation (Fig. 5b) [16,33,34]; opening of a gap (Fig. 5c) [16,24,36,41]; appearance of a negative disclination with a system of stacking faults (Fig. 5d) [16,24]; decomposing a disclination into two others linked by a "disclinational" stacking fault (Figs. 5e and 5f) [16,23]; shifting of the pentagonal axis towards the periphery (Figs. 5g and 5h) [16, 24]; formation of a region without a disclination (Fig. 5i) [16,24]; formation of an open sector outside TBs (Fig. 5j) [16,28]; faceting of the surface near the TBs (Fig. 5k) [21] or around the disclination axis (Fig. 5l) [21,28,42]. In addition, molecular dynamics simulations showed that the core of a disclination in a crystal has a "loose" structure, leading to the formation of an empty channel [43].

For several models, the critical size of pentagonal particles was evaluated (see, for example Refs. [16,33,34]). Starting from the critical size, the relaxation processes in PRs and PPs are triggered by disclinations. Some examples of the aforementioned mechanisms are presented in Fig. 6. The

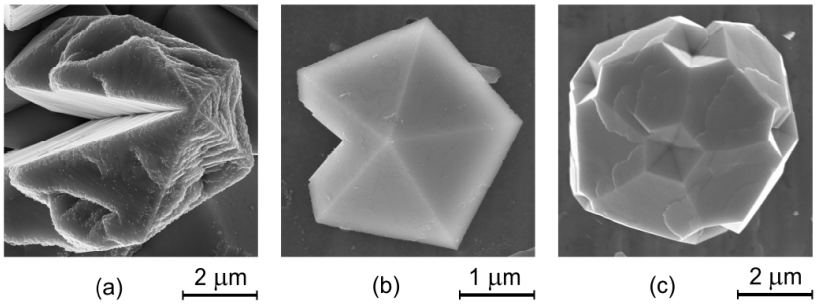

Fig. 6. Examples of relaxation processes in DMCs observed in electrodeposition experiments: (a) opening of a gap instead of TB (Cu DMC); (b) formation of an open sector outside TBs (Ag DMC); (c) faceting surface around the disclination axis (Ag DMC), adapted from [28,41].

details of these mechanisms can be found in the reviews Refs. [16,33,34,38] but, by no means, exhaust all possibilities and modes of internal stress relaxation in DMCs. Recent experiments and their theoretical interpretation revealed new possibilities to reduce the energy associated with the disclination type defect in DMCs. Let us consider the main features of these new results.

a) One of the new mechanism of internal stress relaxation in DMCs is the formation of vacancy prismatic dislocation loops (DLs) in the transverse cross section of DMCs. In [44] for DMCs with decahedral habitus (PRs), it was shown that starting with a certain critical PR radius, the formation of DLs becomes energetically favorable (Fig. 7a). This mechanism was indicative of a threshold character of the phenomenon of nucleation of prismatic DL in PRs. In thin PRs, the DL nucleation is energetically unfavorable, while in PRs with radius larger than the critical one, nucleation becomes possible and the maximum energy gain is achieved for DLs of a certain optimum radius. An energy analysis of the formation of straight dislocations in PRs, has also shown that there is an optimum position of the dislocation relative to the PW axis. It is interesting to note that the relative DL radius corresponding to the maximum energy gain, strongly depends on the critical PR radius for small PRs and virtually reaches saturation for large PRs.

In Ref. [44] it was highlighted that DL formation can be considered as one possible mechanism of the formation of cavities in PRs, which was observed in experiments [35,40]. As it is well known, cavities are formed only during the growth of sufficiently thick PRs and do not appear in thin crystals. This is the evidence for the threshold character of this process, analogous to the considered threshold character of prismatic DL formation. The process of cavity formation with the participation of DLs in PRs can involve the following steps: (i) nucleation of separate vacancy DLs through subtraction along the PR axis (*e.g.*, due to the coagulation of vacancies, which is possible during growth at elevated temperatures); (ii) increase in the density of DLs along the PR axis, which leads to their effective repulsion; (iii) escape of DLs on the outgrowth edge surface with the formation of a trough. Thus, we can envision an imperfection of a PR even before the formation of a visible cavity. Since the optimum DL radius has a non-zero value, the appearance of a finite trough on the edge of a growing PR can be expected starting with a certain critical radius, which was observed in experiments [35,40]

Another aspect of this mechanism was presented in [45] as a stress relaxation in DPs with icosahedral habitus (PPs) through a similar generation of circular prismatic DLs (Fig. 7b). It was shown that loop generation is energetically favorable in the equatorial section of the particle, the radius of which is larger than the critical one. The dislocation loop then extends until it reaches its optimal radius which increases with particle size. Both the critical particle radius and the optimal loop radius strongly depend on the dislocation core energy [45].

b) A new mechanism of internal stress relaxation in DMCs with different habitus was presented in [46-48]. The essence of this phenomenon is that a shell possessing crystal mismatch with respect to the DMC core region (cylinder for PRs [46], sphere for PPs [47]), will reduce the internal energy of the DMC associated with a disclination type defect (Figs. 7c and 7d). The existence of an optimal magnitude for the core/shell crystal lattice mismatch and an opti-

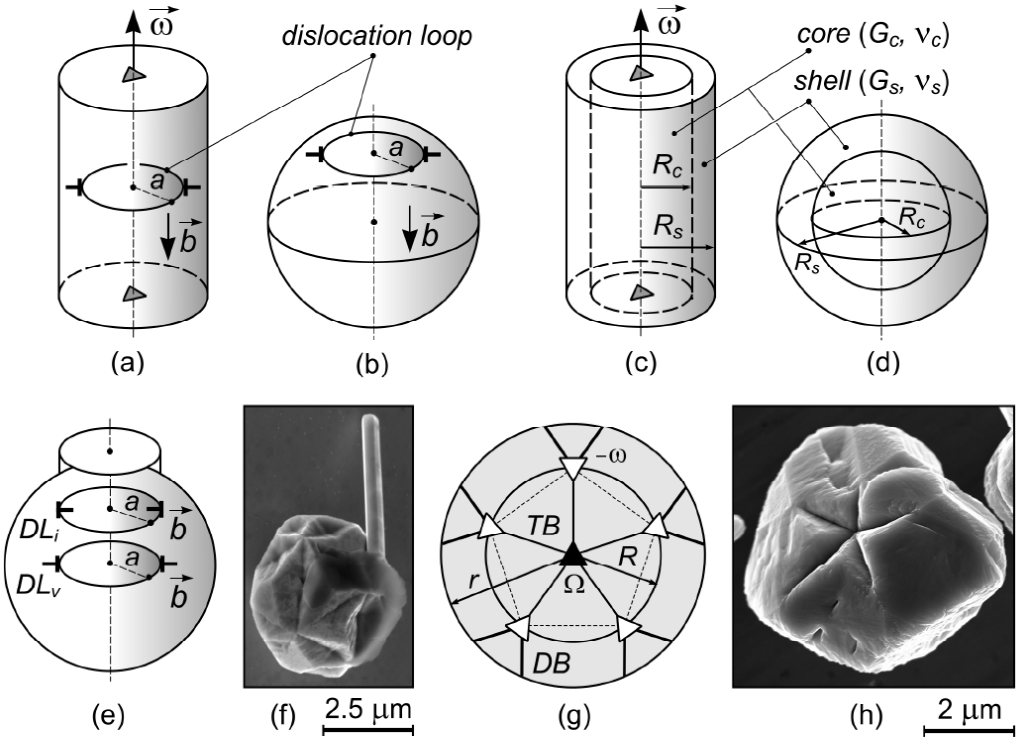

Fig. 7. Recently discussed relaxation processes in DMCs: (a, b) formation of prismatic dislocation loops (DLs) in PR (a) and PP (b); (c, d) formation of a layer with lattice parameter misfit in PR (c) and PP (d); (e, f) outgrowth/extrusion from a DMC; (g, h) formation of screening multi-disclination configurations in DMCs.

mal shell thickness was predicted, providing maximum energy release for this mechanism of mechanical stress relaxation. For PRs, it was pointed out in [46] that the considered relaxation mechanism can be realized by the diffusion of impurities in the shell region without change of the PR radius or by growth of a thin mismatched shell layer with a corresponding thickening of the PR.

Similar considerations for DMC with icosahedral habitus (PPs) gave the value of the critical radius, above which the formation of a layer with lattice parameter misfit is energetically favorable. For typical FCC metals (Cu, Ag), this was of the order of ~10 nm, whereas the corresponding critical radius for DMC with decahedral habitus (PRs) is of the order of ~100 nm [46-48]. The optimal mismatch parameter $\varepsilon^*=(a_{core}- a_{shell})/a_{shell}$, where a_{core} and a_{shell} are the lattice parameters of the core and the shell respectively, gives the maximum energy release at $\varepsilon^*_{opt} \approx -0.01$ for PRs and $\varepsilon^*_{opt} \approx -0.04$ for PPs [46-48].

It should be mentioned that the formation of a circular prismatic misfit dislocation loop in composite core–shell nanoparticles without disclination type defects also becomes energetically favorable if the misfit parameter exceeds a critical value, which is determined by the geometric characteristics of the system [49].

c) Appearance of outgrowths or extrusions from a DMCs can be considered as one of the independent mechanism of internal stress relaxation in DMCs (Figs. 7e and 7f). In Ref. [50], a physical model of outgrowth formation from DMC is presented, which is based upon the notions of nucleation and slippage of prismatic dislocation loops in the elastic field of disclination defects that are inherent in DMCs. The first step of this mechanism is based upon Eshelby's notion [51] that dislocation loops might be involved in the transport of matter from the base to the outgrowth. Internal stresses present in DMCs act as the driving force of the nucleation and propagation of prismatic dislocation loops. Previously, various authors studied the interaction of dislocation loops with isolated wedge disclinations, including the relaxation of stresses in extended prismatic pentagonal crystals [44] and in the vicinity of disclinations emerging at the surface of half-spaces [52]. In the framework of the later model [50], the escape of interstitial dislocation loops at the DMC surface leads to an increase in the whisker length relative to the base, while incorporation of the va-

cancy-type loops is accompanied by their accumulation on the internal surface. This model [50] was illustrated by appropriate calculations that show a gain in the total DMC energy as a result of the formation of a pair of prismatic dislocation loops with opposite signs.

d) Starting from experimental data of Ref. [53], the model of structural changes in DMCs during their growth has recently been developed and subsequently amended in the Refs. [53-55] (Figs. 7g and 7h). In [54], it was shown that after a certain critical size, it becomes energetically favorable for a DMC to form a subsurface layer free of TBs (which are the only typical structural elements for smaller DMC sizes). In this layer, the low-angle dislocation boundaries (DBs) are formed. Calculations of the energy stored in the transformed DMC were based on a disclination model, in which the TB junctions, as well as TB–DB junctions are treated as wedge disclinations. In particular, it was demonstrated that the formation of a TB-free peripheral region becomes energetically possible starting at a particle radius of ~0.04 μm for a disclination of power Ω=0.128 at the center of DMC, with an order of magnitude reduction in power corresponding to particle sizes ~ 0.65 μm.

The multi-disclination configurations with the screening of elastic fields introduced in [54] further interesting extensions in [55], suggest that they are the structure-forming elements of relaxation process for both DMCs and two-dimensional carbon nanostructures. In this sense, the disclination approach has not only been successful to describe two-dimensional carbon structures but also has made it possible to predict new structures taking into account the minimization of the latent energy upon introduction of defects into an initially defect-free carbon film [55].

5. SUMMARY

The structure of DMCs and the elastic distortion of their crystal lattice can be characterized in the framework of the disclination approach. It is the disclination-induced stress relaxation that causes structural transformations in DMCs. Based on experimental observations and theoretical modeling we conclude that there are multiple channels and pathways of stress relaxation and reduction of the elastic energy in DMCs. The realization of a particular relaxation mechanism depends on the environmental conditions including temperature, pressure, presence of oxygen, pH of electrolyte, and other parameters involved in the process of metal electrodeposition.

ACKNOWLEDGEMENT

The authors acknowledge the support of the Ministry of Education and Science of the Russian Federation under the contract no. 14.B25.31.0011 in accordance with the resolution of Russian Government no. 220.

REFERENCES

[1] (a) A.A. Abrikosov // *Introduction to the Theory of Normal Metals*, Nauka, Moscow (1972) 288 p., *in Russian*; (b) J.R. Greer and J.T.M. de Hosson // *Progr. Mater. Sci*. **56** (2011) 654; (c) E.C. Aifantis // *Adv. Appl. Mech*. **49** (2016) 1.
[2] V.G. Gryaznov and L.I. Trusov // *Progr. Mater. Sci*. **37** (1993) 289.
[3] H. Gleiter // *Progr. Mater. Sci.* **33** (1989) 223.
[4] A.D. Yoffe // *Adv. Phys.* **50** (2001) 1.
[5] J. Stangl, V. Holy and G. Bauer // *Rev. Mod. Phys*. **76** (2004) 725.
[6] I.A. Ovidko // *Int. Mater. Rev*. **50** (2005) 65.
[7] W. Lu and Ch.M. Lieber // *J. Phys. D* **39** (2006) R387.
[8] C.C. Koch, I.A. Ovidko, S. Seal and S. Veprek // *Structural Nanocrystalline Materials: Fundamentals and Applications* (Cambridge University Press, Cambridge,2007).
[9] S.V.N.T. Kuchibhatla, A.S. Karakoti, D. Bera and S. Seal // *Progr. Mater. Sci.* **52** (2007) 699.
[10] S. Ino // *J. Phys. Soc. Jap.***21** (1966) 346.
[11] S. Ino and S. Ogawa // *J. Phys. Soc. Jap*. **42** (1967) 1365.
[12] X.Z.Liao, Y.H. Zhao, S.G. Srinivasan, Y.T. Zhu, R.Z. Valiev and D.V. Gunderov // *Appl. Phys. Lett.* **84** (2004) 592.
[13] X.H. An, Q.Y. Lin, S.D. Wu, Z.F. Zhang, R.B. Figueiredo, N. Gao and T.G. Langdon // *Scripta Mater.* **64** (2011) 249.
[14] L.D. Marks // *Rep. Prog. Phys.* **57** (1994) 603.
[15] H. Hofmeister // *Cryst. Res. Technol.* **33** (1998) 3.
[16] V.G. Gryaznov, J. Heidenreich, A.M. Kaprelov, S.A. Nepijko, A.E. Romanov and J. Urban // *Cryst. Res. Technol*. **34** (1999) 1091.
[17] M.J. Yacaman, J.A. Ascencio, H.B. Liu and J. Gardea-Torresday // *J. Vac. Sci. Technol. B* **19** (2001) 1091.
[18] Z. Tang and N. A. Kotov // *Adv. Mater.* **17** (2005) 951.
[19] A.A. Vikarchuk and I.S. Yasnikov, *Structure formation in nanoparticles and microcrystals*

with pentagonal symmetry formed during metal electrocrystallization (Togliatti State University Press, Togliatti, 2006), *in Russian*.
[20] Y. Xia, Y. Xiong, B. Lim and S.E. Skrabalak // *Angew. Chem. Int. Ed. Engl*. **48** (2009) 60.
[21] L.D. Marks and L. Peng // *J. Phys.: Condens. Matter.* **28** (2016) 053001.
[22] K. Koga and K. Sugawara // *Surf. Sci.* **529** (2003) 23.
[23] A.A. Vikarchuk and A.P. Volenko // *Phys. Solid State* **47** (2005) 352.
[24] I.S. Yasnikov // *Tech. Phys. Lett.* **52** (2007) 666.
[25] D. Seo, C.I. Yoo, I.S. Chung, S.M. Park, S. Ryu and S. Hyunjoon // *J. Phys. Chem. C* **112** (2008) 2469.
[26] C.R. Li, N.P. Lu, Q.Xua,J. Mei, W.J. Dong, J.L. Fu and Z.X. Cao // *J. Cryst. Growth* **319** (2011) 88.
[27] A.E. Romanov, A.A. Vikarchuk, A.L. Kolesnikova, L.M. Dorogin, I. Kink and E.C. Aifantis // *J. Mater. Res*. **27** (2012) 545.
[28] I.S. Yasnikov, M.V. Dorogov, M.N. Tyurkov, A.A. Vikarchuk and A.E. Romanov // *Cryst. Res. Technol.* **50** (2015) 289.
[29] W. Ji, W. Qi, X. Li, S. Zhao, S. Tang, H. Peng and S. Li // *Mater. Lett*.**152** (2015) 283.
[30] J. Helmlinger, O. Prymak, K. Loza, M. Gocyla, M. Heggen and M. Epple // *Cryst. Growth Des.* **16** (2016) 3677.
[31] R. De Wit // *J. Phys. C* **5** (1972) 529.
[32] J.M. Galligan // *Scripta Met.* **6** (1972) 161.
[33] A. E. Romanov and A. L. Kolesnikova // *Progr. Mater. Sci.* **54** (2009) 740.
[34] V.G. Gryaznov, A.M. Kaprelov, A.E. Romanov and I.A. Polonsky // *Phys Stat. Sol. (b)* **167** (1991) 441.
[35] I.S. Yasnikov and A.A. Vikarchuk // *Phys. Solid State* **48** (2006) 1433.
[36] I.S. Yasnikov and D.A. Denisova // *Phys. Solid State* **55** (2013) 642.
[37] A.A. Vikarchuk, N.N. Gryzunova, M.V. Dorogov, A.N. Priezzheva and A. E. Romanov // *Metal Sci. Heat Treat.* **58** (2016) 12.
[38] A.E. Romanov and V.I. Vladimirov, In: *Dislocations in solids*, ed. by F.R.N. Nabarro vol. 9. (North-Holland, 1992).
[39] A. Howie and L. D. Marks // *Phil. Mag. A* **49** (1984) 95.
[40] A.E. Romanov, I.A. Polonsky, V.G. Gryaznov, S.A. Nepijko, T.Junghanns and N.I. Vitrykhovski // *J. Cryst. Growth* **129** (1993) 691.
[41] I.S. Yasnikov // *JETP Lett.* **97** (2013) 513.
[42] I.S. Yasnikov // *Tech. Phys. Lett.* **34** (2008) 944.
[43] A.I. Mikhailin and A.E. Romanov // *Sov. Phys. Solid State* **28** (1986) 337.
[44] A.L. Kolesnikova and A.E. Romanov // *Tech. Phys. Lett.* **33** (2007) 886.
[45] M.Yu. Gutkin, A.L. Kolesnikova, S.A. Krasnitckii, L.M. Dorogin, V.S. Serebryakova, A.A. Vikarchuk and A.E. Romanov // *Scripta Mater.* **105** (2015) 10.
[46] A.L. Kolesnikova and A.E. Romanov // *Phys. Stat. Sol. RRL* **1** (2007) 271.
[47] L.M. Dorogin, A.L. Kolesnikova and A.E. Romanov // *Tech. Phys. Lett*. **34** (2008) 779.
[48] L.M. Dorogin, S. Vlassov, A.L. Kolesnikova, I. Kink, R. Lohmus and A.E. Romanov // *Phys. Stat. Sol. B* **247** (2010) 288.
[49] M.Yu. Gutkin, A.L. Kolesnikova, S.A. Krasnitsky and A.E. Romanov // *Phys. Solid State* **56** (2014) 723.
[50] A.E. Romanov, L.M. Dorogin, A.L. Kolesnikova, I. Kink, I.S. Yasnikov and A.A. Vikarchuk // *Tech. Phys. Lett.* **40** (2014) 174.
[51] J. D. Eshelby // *Phys. Rev.* **91** (1953) 755.
[52] A.A. Vikarchuk, N.N. Gryzunova, O.A. Dovzhenko, M.V. Dorogov and A.E. Romanov // *Adv. Mater. Res.* **1013** (2014) 205.
[53] I.S. Yasnikov // *Tech. Phys. Lett.* **40** (2014) 411.
[54] I.S. Yasnikov, A.L. Kolesnikova and A.E. Romanov // *Phil. Mag. Lett.* **95** (2015) 450.
[55] I.S. Yasnikov, A.L. Kolesnikova and A.E. Romanov // *Phys. Sol. State* **58** (2016) 1184.